Functionally graded biomaterials for use as model systems and replacement tissues

**Jeremy M. Lowen**[1], **J. Kent Leach**[1,2,*]

[1]Department of Biomedical Engineering, University of California, Davis, CA, 95616

[2]Department of Orthopaedic Surgery, UC Davis Health, Sacramento, CA 95817

Abstract

The heterogeneity of native tissues requires complex materials to provide suitable substitutes for model systems and replacement tissues. Functionally graded materials have the potential to address this challenge by mimicking the gradients in heterogeneous tissues such as porosity, mineralization, and fiber alignment to influence strength, ductility, and cell signaling. Advancements in microfluidics, electrospinning, and 3D printing enable the creation of increasingly complex gradient materials that further our understanding of physiological gradients. The combination of these methods enables rapid prototyping of constructs with high spatial resolution. However, successful translation of these gradients requires both spatial and temporal presentation of cues to model the complexity of native tissues that few materials have demonstrated. This review highlights recent strategies to engineer functionally graded materials for the modeling and repair of heterogeneous tissues, together with a description of how cells interact with various gradients.

Graphical Abstract
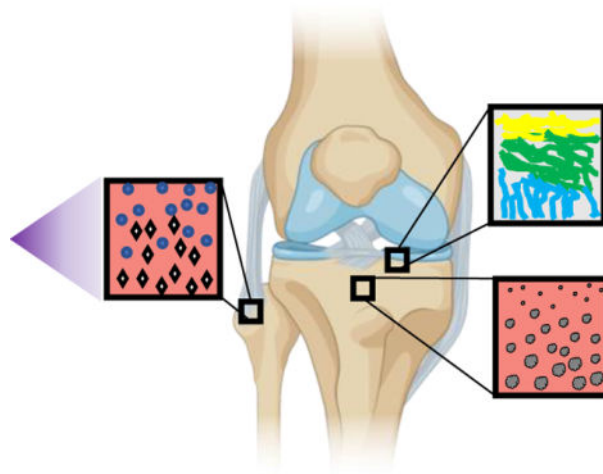
*Address for correspondence: J. Kent Leach, Ph.D., Department of Biomedical Engineering, University of California, Davis, 451 Health Sciences Drive, Davis, CA 95616, jkleach@ucdavis.edu.

Disclosure
The authors have no conflict of interest.

The heterogeneity of native tissues requires complex materials to provide suitable substitutes for model systems and replacement tissues. Advancements in microfluidics, electrospinning, and 3D printing enable the creation of functionally graded materials that have the potential to address this challenge by mimicking the gradients in tissues such as porosity, mineralization, and fiber alignment to influence strength, ductility, and cell signaling.

Keywords

Gradient materials; light-based gradients; composites; tissue engineering; mesenchymal stromal cells

Table of Contents keyword

Gradient materials

1. Introduction

Gradient-based biomaterials are an exciting advancement in the field of materials science and tissue engineering that are designed to mimic naturally occurring gradients in composition, signaling cues, and other constituents found *in vivo*. The advancement of technologies such as dynamic biomaterials, 3D bioprinters, and stem cell programming has fueled the growth of the tissue engineering field. Functionally graded materials (FGMs) represent one such advancement where biomaterials are designed to imitate the natural heterogeneity found in tissues throughout the body. In their simplest form, FGMs are composed of two constituent materials or phases which spatially change from one to the other. FGMs were first investigated in the 1980s for the design of heat-resistant materials for spacecraft that could withstand high temperature gradients (temperatures up to 2000 K with a gradient of 1000 K).[1] Thereafter, the benefits of non-homogeneous materials have been exploited to design materials with specific structural, chemical, and morphological characteristics to influence mechanical properties and cell signaling.

Mechanical and biochemical gradients are found throughout the body and provide structural integrity at transitional interfaces of tissues (Figure 1). Bone is one example of a natural gradient in both radial and longitudinal directions. In the radial direction, bone consists of a dense outer structure (cortical bone) that changes to a softer and more porous internal material (cancellous bone).[2] Longitudinally, bone is composed of collagen fibers aligned to bear the necessary compressive and torsional forces to enable locomotion, resist mechanical stresses, and provide protection for internal organs. By varying its structural properties, bone can withstand external loading while enabling the transportation of nutrients and waste. Tendon-to-bone integration exhibits spatial variations in mineral concentration and collagen fiber orientation that enables efficient force transmission while minimizing stress.[3] Articular cartilage is yet another highly graded tissue interface where collagen fibers are aligned parallel to the articular surface and are increasingly perpendicular as they approach subchondral bone.[4] Gradients are evident in cell signaling as well, with cells migrating in response to gradients of soluble chemoattractants, surface-attached molecules, and stiffness.

[5] Thus, gradients in stimuli, whether derived from composition, mechanical forces, or soluble cues, have an important effect on tissue development, regeneration, and homeostasis.

The design of FGMs have the potential to recreate the biological function of these heterogeneous tissues and increase our understanding of how to integrate biomaterials *in vivo*. The variety of techniques employed to form FGMs often utilize homopolymers, copolymers, or composite materials to create FGMs with a wide range of properties. This review will describe recent advances in the field of FGMs and how they are applicable for new models of tissue development, repair, and for replacement tissues.

2. Methods for the fabrication of functionally graded materials

Gradients of composition, porosity, stiffness, and biochemical concentration are among the most frequently studied due to their known effects on cell behavior. Gradients may be continuous or discrete and extend in a linear or non-linear fashion. Scaffolds for softer tissues will often use more compliant biomaterials such as hydrogels, while harder tissue substitutes make increased use of stiff, slowly resorbing polymers and ceramics due to their ability to withstand higher mechanical load. With the increased use of FGMs in tissue engineering, several methods have been developed for incorporating gradients into biomaterials including light-based methods, 3D printing, microfluidics, electrospinning, freeze-drying, and solvent casting/particulate leaching (Table 1). The following section will discuss the fabrication of FGMs using these common methods.

2.1 Light-based methods

Light-based methods for the synthesis of materials and gradients rely on the incorporation of a photosensitive component, whereupon exposure to a designated wavelength initiates a chemical reaction that results in the formation or disintegration of crosslinking bonds. Hydrogels, highly tailorable polymeric networks capable of absorbing high amounts of water (70–99%),[6] are widely used as photoresponsive substrates.[7] Hydrogels are appealing due to their capacity to mimic the fibrous and viscoelastic characteristics of the native extracellular matrix (ECM), as well as their hydrated nature and biocompatibility. Hydrogels are derived from natural proteins or polysaccharides such as collagen, fibrin, or alginate, or synthetic polymers such as polyethylene glycol (PEG), polyacrylamide (PA), and polyvinyl alcohol (PVA) to name a few. These polymers can be functionalized to respond to light, chemicals, pH, ionic concentration, temperature, and magnetic and electrical fields.[8] Furthermore, these materials may be engineered to be hydrolysable or degradable over time and have tunable biophysical properties through manipulation of crosslinker concentration, applied wavelength, and duration of irradiation.

Photolithography is useful for creating gradients by regulating the light that reaches a photolabile material. A photomask controls the distribution of light based on regions of translucency, providing the opportunity to dictate crosslinking down the axis (Figure 2A).[9] PA gels were formed with opposing gradients of stiffness and protein concentration using photolithography.[10] Gradient photomasks were designed with translucent regions to allow light penetration and opaque regions to attenuate light transmission. Polymerization was initiated by Irgacure 2959 and exposure to 254 nm UV light. Gel crosslinking correlated

with the design of the photomask and resulted in soft and stiff regions ranging from 46.7 kPa to 126.7 kPa. When fibroblasts were seeded on gradient gels, cells preferentially migrated towards the stiffer end of the gel. Immobilized collagen gradients were then created by conjugating type 1 collagen to the PA gels using N-hydroxyl succinimide (NHS) and sulfo-succinimidyl-diazirine (SDA) chemistry. The collagen was exposed to 365 nm UV light, which superimposed an opposing collagen gradient on top of the rigidity gradient. When combining opposing mechanical and biochemical gradients, fibroblast migration was reversed toward the softer elastic modulus and higher collagen concentration. Human mesenchymal stromal cells (MSCs) followed a similar trend of migrating up a stiffness gradient when seeded on collagen-coated PA gels.[11] Adipose derived stromal cells (ASCs) were entrapped within a gelatin methacryloyl (GelMA) hydrogel with a continuous stiffness gradient.[12] ASCs seeded in low stiffness regions (~8 kPa) exhibited increased cellular and nuclear volume and enhanced mechanosensitive protein localization in the nucleus, while the reverse was seen high stiffness regions (~30 kPa). Conversely, when ASCs were seeded on top of a gradient PA hydrogel, ASCs exhibited more cell spreading and nuclear localization of Lamin A and YAP at higher stiffnesses (Figure 2C).[13]

As an alternative to photomasks that are fixed to control light transmission, the mask can be pulled across the biomaterial to create a spatiotemporal gradient of UV exposure time (Figure 2A).[14] Methacrylated hyaluronic acid (HA) hydrogels with stiffness ranging from 3 to 100 kPa were produced and seeded with human MSCs.[15] Cells exhibited increased spreading and proliferation on the stiffer regions compared to MSCs on softer portions of the gels. Stiffness gradients were produced in PA gels from 1–240 kPa using a similar technique. [16] Beyond manipulating hydrogel mechanical properties alone, polymers such as polyethylene glycol monoacrylate (PEGMA) have been used to create hydrogels with accelerated degradation that correspond to increased UV exposure time.[17] Surface charge has also been controlled with photomask-generated gradients. Sulfhydryl-to-sulfonate surface gradients were created by sliding a mask over a surface functionalized with 3-mercaptopropyltrimethoxysilane (MTS), which oxidized an increasing amount of thiol groups with longer exposure time.[18] Solutions of platelet free plasma (PFP), fibrinogen, and albumin were then washed over the surface to observe the combined effect of surface charge and the nature of the adsorbed protein on platelet adhesion. Surface charge gradients adsorbed with PFP promoted adhesion that was inversely related to the negative surface charge density, gradients with fibrinogen showed maximum adhesion in the center, and gradients with albumin resulted in low overall adhesion.

As an alternative to traditional photomasks, maskless photolithography is achievable with projection photolithography. A UV light source illuminates a digital micromirror device that uses an array of fluctuating mirrors to regulate the output intensity of light of the desired image to be projected.[19] Compared to mask-based photolithography, this method only requires an 8-bit image grayscale image and is not limited to the resolution or movement of a photomask. This system can be used with both photocrosslinkable and photodegradable hydrogels to create stiffness gradients with submicron resolution or pattern distinct regions of hydrogels for functionalization.[19–20]

Photon irradiation has been increasingly employed to generate light-based gradients since the discovery of two-photon irradiation in 1990.[21] Two-photon photolithography uses a highly focused laser beam that raster scans material and may be used to efficiently cleave coumarin-derived photocages.[22] 6-bromo-7-hydroxy coumarin (Bhc) is a common photocaging molecule used to protect amines and thiols. Upon activation, Bhc can immobilize gradients of molecules such as maleimide-functionalized growth factors (*e.g.*, vascular endothelial growth factor, VEGF).[22–23] As a model of angiogenesis, endothelial cells migrated into gels with VEGF gradients, but no migration was observed with gels lacking immobilized VEGF or without a gradient (*i.e.*, homogeneously immobilized VEGF). [22]

Photolabile crosslinkers are often used when mixing two distinct hydrogel precursor solutions to create a continuous gradient between two solutions. These solutions may be mixed at different rates using a syringe or peristaltic pump, pumped into a glass mold, and the resultant graded solution is crosslinked by exposure to light.[24] Flow rates vary from 0–50 mL/h with flow rates on the lower end (~100 μL/min) used to prevent mixing of the gradient before crosslinking. Constructs typically range from 50–500 mm^3 but can vary widely depending on application.[25] Gradients of stiffness within a copolymer hydrogel have been created by loading polymers of different molecular weight into each syringe, while hydrogels presenting gradients in peptide presentation (*i.e.*, HAVDI, which mimics N-cadherin) were created in a similar fashion.[26] Methacrylated alginate hydrogels possessing gradients of stiffness and adhesive peptide (RGD, Arg-Gly-Asp) concentration were seeded with MSCs to test the role of multiple interactions on cell differentiation and proliferation. [25b] More MSCs were observed in regions of lower stiffness and higher RGD concentration. Gradients of short interfering RNA (siRNA) have also been formed to spatially control gene expression, showcasing the versatility of biological processes applicable to this platform. [25a] In particular, human embryonic kidney (HEK293) cells transfected with destabilized green fluorescent protein (deGFP) displayed a gradient of fluorescence intensity upon spatial presentation of deGFP siRNA.

While homopolymers may be mixed at different rates, interpenetrating network (IPN) hydrogels can be formed by mixing two monomers that polymerize independently when exposed to different light sources. Acrylate and epoxy monomers were mixed with radical and cationic photoinitiators to create functionally graded IPNs by spatial exposure to different wavelengths of light.[27] Scaffolds with porosity gradients have also been created by combining organic (polyethylene glycol diacrylate, PEGDA) and inorganic (methacrylated star polydimethylsiloxane, PDMS$_{star-MA}$) macromers and suspending them in aqueous or organic solvents after crosslinking.[28] These gradient scaffolds exhibited swelling values from 5.5 to 12, stiffnesses of 40 to 405 kPa, and the ability to spatially control PDMS$_{star-MA}$ distribution, pore size, and bioactivity, which could be utilized for rapid screening of cell-material interactions.

Photocrosslinking may be used to use fuse independent hydrogel solutions and form a discrete gradient by stacking crosslinked layers (Figure 2B). A prehydrogel solution of PEGDA or GelMA was deposited inside a PDMS well and crosslinked by exposure to UV light. The next layer was deposited on top and crosslinked in the same manner. Each layer

can be composed of different concentrations of biomolecules or hydrogels to effectively create a gradient across the finished construct.[29] Fibroblasts migrated and exhibited distinct morphologies on these materials possessing a stiffness gradient, with cells on more compliant areas remaining round while cells on stiffer regions becoming more spindle-like.[29]

Light-based gradient fabrication utilizes methods with high resolution and facilitates high throughput formation. The light-responsive photoinitiator functions through the generation of free radicals that crosslink macromers, yet this approach may impair cell or DNA damage due to UV light.[30] Common photoinitiators include Irgacure 2959 and Irgacure 1173. Irgacure 2959 is most common due to its high free radical generation efficiency and higher water solubility.[31] Careful modulation of UV and photoinitiator exposure must be maintained to prevent cell damage.

2.2 3D Printing

3D printing is an exciting approach to create complex structures with more biocompatible, and even cell-loaded, materials that were previously required to be formed by micromachining or with sacrificial polymers. 3D printing can generate FGMs by precisely depositing materials based on predesigned models.[32] There are multiple types of bioprinters including inkjet printers which use air pressure or mechanical pulses to eject droplets of polymer or bioink and microextrusion printers which employ pneumatic, piston, and screw-based mechanisms to produce flow of bioink.[33] Continuous Liquid Interface Production (CLIP) printers utilize carefully controlled oxygen inhibition and UV curable resin to rapidly extrude constructs from a resin vessel[34], while freeform reversible embedding of suspended hydrogels (FRESH) printers use a thermoreversible support bath to print hydrogels in complex, 3D structures.[35] Bioprinters can be used with a variety of materials including hydrogels, synthetic polymers that can be readily extruded, and ceramics (Table 2).

Poly(ε-caprolactone) (PCL) is a synthetic polymer commonly used for printing due to its biocompatibility, processability, and ease in forming gradients.[36] For example, PCL fibers were photochemically decorated with propargyl benzophenone using a gradient photomask and an azide-modified IKVAV peptide to guide neuronal cell growth.[37] Unlike PCL fibers lacking a gradient, neuronal cells exhibited increased alignment and migration up the peptide gradient of IKVAV-gradient PCL fibers. Polylactic acid (PLA) and poly(ethyleneoxide terephthalate)/ poly(butylene terephthalate) (PEOT/PBT) copolymers are also popular due to their physico-chemical properties, safety profile, and regulatory approval for orthopedic applications.[38] These polymers were sequentially deposited to create surface energy and stiffness gradients for osteochondral regeneration.[38] As surface energy increased, more proteins were adsorbed, forming more anchor points for cells and instructing their final shape and degree of spreading. PCL scaffolds were printed in the shape of sheep menisci and loaded with connective tissue growth factor (CTGF) and transforming growth factor-β3 (TGFβ3) to induce recruitment and fibrochondrocytic differentiation of endogenous cells.[39] Compared to non-loaded scaffolds, the treatment group resulted in superior meniscus regeneration with zonal properties. PCL has also been

used in combination with collagen for interfacial tissue engineering to resemble the transition between tissues.[40] PCL fibers were printed to form scaffolds with a pore size of 200 μm, followed by controlled immersion of the scaffolds in a 1,6 hexanediamine/isopropanol solution in order to create an amine (NH_2)-density gradient along the length of the substrate. The scaffolds were subsequently covered with collagen *via* carbodiimide chemistry, which promoted adhesion of cells on the scaffolds and induced increases in metabolic activity up the collagen gradient.

Collagen is a common choice for cartilage tissue engineering due to its prevalence in native cartilage, as well as its high biocompatibility and ability to support cell adhesion. Collagen was printed at different concentrations to alter the compressive modulus from <1 kPa to 30 kPa without affecting cell viability.[50] In an effort to replicate the zonal distribution of cartilage that is present *in vivo*, collagen type II was sequentially printed with increasing chondrocyte density.[51] Alginate is another common hydrogel used in biofabrication due to its biocompatibility, low cost, and gelation under mild conditions.[52] Gradients in pore size within alginate were formed for spatiotemporal gene delivery by modulating the ratio of methylcellulose to alginate and washing the methylcellulose out post-fabrication.[45] By controlling porosity, the investigators achieved both rapid and transient transfection of osteogenic and chondrogenic genes to induce complex tissue formation such as the bone-soft tissue interface. Porosity gradients were also created in an IPN of alginate and gelatin with pore sizes ranging from 80–2125 μm, demonstrating the potential of 3D printing in developing bio-based scaffolds with controlled pore size.[53]

Ceramics are commonly used to form engineered tissues such as bone, as these carbonated phosphates can withstand high temperatures, abrasion, and mechanical stresses.[54] Functionally-graded ceramics are promising for use in the transition zone between the chondral and osseous phases at the bone-cartilage interface. Gradients of β-tricalcium phosphate (β-TCP) were printed with a potent, chondroinductive growth factor (transforming growth factor beta 1, TGF-β1) in a poly(N-acryloyl glycinamide) (PNAGA) gel to promote osteogenic and chondrogenic differentiation of human MSCs.[46] Hydroxyapatite (HAp) is another calcium phosphate (CaP)-based ceramic that has been 3D printed for use at the osteochondral interface. HAp was combined with PCL to fabricate constructs with gradients in composition and porosity.[44] These scaffolds demonstrated an inverse relationship between porosity and compressive modulus that was independent of ceramic concentration. By inclusion of the ceramic phase, these scaffolds had an average compressive modulus between 86 – 220 MPa, which is within the physiological range of trabecular bone. GelMA is a photo-crosslinking bioink that can be combined with ceramics to create gradient constructs. A GelMA/HAp tri-layered scaffold was fabricated with increasing concentrations of GelMA and HAp in each layer and implanted in a rabbit osteochondral defect.[55] Compared to a monophasic scaffold, the tri-layered scaffold resulted in faster cartilage regeneration. Bioactive glass (BG) is a ceramic that releases ions which promote cell adhesion, proliferation, and differentiation.[56] A gradient scaffold consisting of a top layer of poly(N-acryloyl 2-glycine) (PACG)-GelMA-Mn^{2+} and bottom layer of PACG-GelMA-BG was 3D printed for osteochondral repair.[57] After implantation in a rat osteochondral defect, subchondral bone formation in the gradient scaffold was significantly greater compared to scaffolds without Mn^{2+} and BG. These findings

demonstrate the promise of producing gradient materials that may have utility in modeling or replacing damaged interfacial connective tissues.

Inkjet printing can create functionally graded ceramic structures in a more continuous fashion compared to additive manufacturing. Complex 3D geometries of alumina and zirconia powder-based inks were inkjet printed in an effort to provide better control over material combinations.[58] This experiment illustrated the potential to create a smooth transition between multiple ceramics with high accuracy with regard to drop positioning. Inkjet printing can also be used to create gradients of growth factors on substrates.[59] Gradients of basic fibroblast growth factor (FGF-2) and bone morphogenetic protein-2 (BMP-2) were printed on coverslips to test the capacity of growth factor combinations to promote osteogenic differentiation of the murine multipotent C2C12 cell line.[60] FGF-2 had an inhibitory effect on osteogenic differentiation, while ALP expression was highest in BMP-2 only conditions that increased up the concentration gradient. Growth factor gradients have also been generated by creating a gradient of heparin-binding domains to attract heparin-binding growth factors (HBGFs) such as FGF-2. Gradients in heparin-binding domains were created in hyaluronate-based hydrogels with heparin sulfate proteoglycan-derived perlecan/HSPG2 domain I (Figure 3B).[61] MC3T3 pre-osteoblasts and MDA-MB-231 breast cancer cells migrated up a FGF-2 gradient formulated using 3D printing.

Bioprinting facilitates rapid, on-demand prototyping of constructs possessing complex architectural and chemical cues. Printing in three dimensions enables formation of increasingly complex gradients, with the ability to integrate multiple materials by employing multiple print heads. However, materials utilized in 3D printing must be viscous enough to maintain structure post-printing but be shear-thinning to enable extrusion from the print head.[62] Post-processing may also be necessary to remove support material or facilitate crosslinking.

2.3 Microfluidics

Microfluidic platforms capitalize on their precise control of fluid flow to generate gradients of bioactive factors and shear stress, which provide the opportunity to study model systems *in vitro* on a miniaturized scale. Such platforms can be combined with other technologies such as 3D printing and electrospinning to produce highly tailored gradient scaffolds. Their small scale facilitates high-throughput analysis at the single cell level, significantly reduces reagent cost, and provides highly responsive dynamic gradients by modulating flow rates.[63] A large portion of microfluidic devices are fabricated through soft lithography techniques and utilize polydimethylsiloxane (PDMS) as their substrate.[64]

Microfluidic systems are under development to model biochemical gradients that are observed *in vivo* and study their effect on cell behavior. Microfluidic gradients can be generated using tree-shape devices, Y-shape devices, membrane-based devices, pressure balance, droplet generation, and others.[63] Embryonic stem cells (ESCs) were exposed to orthogonal gradients of morphogens to promote localized differentiation of motor neurons in the neural tube, while a rotating gradient was applied to highly metastatic fibrosarcoma HT1080 cells to influence migration.[65] Microfluidic devices facilitate the application of non-linear concentration gradients that are involved in cell migration, differentiation, and

growth.[66] Asymmetrical grids of channels promoted nonlinear diffusion that creates exponential and sigmoidal gradients.[66] The applicability of this design was demonstrated by assessing fibroblast cell viability in response to non-linear hydrogen peroxide (H_2O_2) concentrations.

Bilayered microfluidic devices have been used to guide the differentiation of stem and progenitor cells *in vitro*. Within a bilayered microfluidic device, MSCs were suspended in agarose in the bottom compartment, which was separated by a microporous membrane from the top layer that contained 3 media channels for growth, osteogenic, and chondrogenic media.[67] This design exposed the cells to a gradient of soluble cues due to the mixing of the three media channels after diffusion through the membrane. Osteogenesis was achieved in cells exposed primarily to osteogenic media, while those cells stimulated by chondrogenic media primarily underwent chondrogenesis. Cells exposed to the middle of the device exhibited a gradient of differentiation between the two lineages. A similar bilayered device was created with the addition of decellularized omentum ECM to the bottom of the device to serve as a scaffold.[68] The addition of natural ECM further recapitulates the complexity of the natural 3D microenvironment, providing an opportunity to use microfluidics to better model native tissues.

Biochemical gradients can be combined with mechanical gradients to interrogate the additive and synergistic effects of stimuli on cell behavior and function. Fibroblasts seeded on nanofibers of different spacings in a microfluidic device were sensitive to platelet-derived growth factor (PDGF-BB) dose.[69] Fibroblasts underwent maximal chemotaxis at lower PDGF doses and closer nanofiber spacing, which enabled cells to spread over two fibers and have punctate sites of adhesion. Gradients of substrate stiffness may also be formed within microfluidic devices to explore the synergistic influence of chemical concentration and ECM compliance on cell function. Orthogonal chemical and rigidity gradients were obtained by mixing PA solutions with different chemical concentrations in a microfluidic device. The solutions were blended at a Y-junction and subsequently irradiated while sliding a photomask over the device.[70] The liquid pressure of cell-laden hydrogels resulted in convex PDMS deformations in the center of a microfluidic device, and UV patterning was applied to create a height gradient under the PDMS.[71] When excess fluid was removed, the PDMS membrane flattened, applying increasing force towards the center of the device and generating a compressive force gradient. Porosity gradients are yet another form of stimuli attainable with microfluidics. The pore size in alginate nanogels was regulated by altering flow rates in the channel containing the monomer and the channel containing the $CaCl_2$ crosslinker.[72] Nanogel diameter varied from 68–138 nm and pore size ranged from 11–24 nm. This technology could be utilized to tailor release rates of polypeptides or other compounds from the hydrogel. PEG microgels were fabricated and annealed to form a gradient in stiffness. Human MSCs seeded on the microgel scaffold exhibited increased proliferation and spreading up the stiffness gradient (Figure 3A).[73]

Gradients created within microfluidic devices are useful to mimic native physiology on a small scale. For example, an oxygen gradient ranging from 2% to 21% was created to investigate the influence of oxygen tension on gene expression and metabolism on human ESC-derived hepatocytes.[74] One side of a microfluidic device was exposed to a channel of

a continuously flowing 95% N_2/5% CO_2 gas mixture to generate the oxygen gradient. Oxygen gradients were also created by infusing sodium sulfite, an oxygen scavenger, through a microfluidic device.[75] When the device was loaded with endothelial cells and fibroblasts, biased vessel growth toward the scavenger channel was observed in both chronic and intermittent hypoxia conditions. Thus, precise spatiotemporal gradients of oxygen are created by leveraging the minimal diffusion distance oxygen must travel in microfluidic devices and regulating fluid flow through the microdevices.

Microfluidic gradients are valuable to test the effect of chemical concentrations on cells in a high-throughput manner. Microfluidic chambers were created by overlapping PDMS layers to form grid-like channels used to test antimicrobial susceptibility.[76] *E. coli* was seeded in the device and exposed to a unique concentration of ampicillin and gentamicin at each intersection, thereby enabling efficient testing of antibiotic doses with minimal reagents. The bacterial burden was minimized at intersections containing high doses of both antibiotics, demonstrating the synergistic effect of the drugs. In another example, microfluidic systems were used to study the efficacy of a colorectal cancer treatment, demonstrating increasing cell death up the concentration gradient.[77] This is a valuable tool for determining both effective dose and diffusive properties of drugs. Alternatively, microfluidic devices can model gradients of cytotoxic chemicals and their dose-dependent effect on cells. Microfluidic devices were used to mimic environmental pollution by applying a gradient of benzopyrene to bronchial epithelial cells in a model of lung pathophysiology.[78] The benzopyrene directionally induced cell shrinkage, cytoskeleton disintegration, reactive oxygen species (ROS), and inflammatory cytokines in the bronchial epithelium.

Cell migration, a process dependent on adhesivity, cell density, and chemotactic signals, can be studied utilizing gradients created in microfluidic devices. A gradient of laminin oligopeptide concentration was generated in an H-shaped microfluidic network between channels containing peptide-grafted collagen or untreated collagen.[79] The migration of chick dorsal root ganglion neurons was observed between the channels and in response to laminin peptides. Similarly, growth factor gradients were created in a 3D microfluidic device to interrogate osteoblast chemotaxis in bone regeneration.[80] A microfluidic chip was developed for studying the responsiveness of lung cancer cells to phototaxis, the migration of cells or organisms toward or away from light.[81] A light-gradient chip was laser inscribed and placed on top of a cell-culture chip with blue light illuminating the top. Lung cancer cells migrated to the darker side of the chip due potentially to the production of intracellular ROS proportional to the intensity of blue light.

Microfluidic chips can be combined with other technology to produce complex gradient scaffolds. A microfluidic device was designed with a valve-based flow-focusing junction (vFF), in which the size of the orifice was adjusted in real time by thin pressurized PDMS walls.[82] This device was then connected to an extrusion printer to manufacture 3D scaffolds with varying porosity achieved by adjusting the valve diameter of the microfluidic device. In another example, a Y-junction microfluidic device was combined with electrospinning to produce nanofibers with a gradient of nanoparticles and biomolecules.[83] Microfluidic platforms provide a technique to create highly reproducible gradients with small reagent volumes. These devices are useful to study single cell responses to functional

gradients or to create precise gradients on a larger scale when combined with other technologies. However, microfluidics introduce non-standard cell culture techniques that require familiarization and limit experiments to relatively small volumes compared to conventional cell culture. Therefore, microfluidics represent an excellent platform to investigate specific cell-cell or cell-environment interactions but may not be appropriate for large scale studies.

2.4   Electrospinning

Electrospinning exploits the electrostatic repulsion between surface charges to continuously draw nanofibers from a viscoelastic fluid.[84] Importantly, the fibers produced with polymers, ceramics, and small molecules possess dimensions on the nanometer scale, similar to the native ECM.[85] The resulting fibers can be functionalized and aligned, making electrospinning an appealing choice for producing FGMs.[86]

Electrospinning can create a substrate with gradients in various morphological and mechanical properties simply by dispersing one layer, changing the syringe to one containing a different material, and then depositing the next layer on top. Bilayer scaffolds were created by consecutively spinning polyhydroxybutyrate-co-hydroxyvalerate (PHBV) to generate nanofibers, followed by PLA or PCL to produce microfibers.[87] The scaffold was inverted and another layer of microfibers was deposited, resulting in a trilayered scaffold with a nanofibrous middle structure. The PHBV nanofibers acted as a barrier membrane permeable to nutrients but blocking cell migration, while the microfibers supported cell proliferation. A PLA-PCL-collagen trilayered scaffold was synthesized in a similar fashion for use as a dural substitute.[43] The inner layer of PLA was incorporated to prevent tissue adhesion, the midlayer with PCL to provide a watertight seal, and the outer layer of collagen to promote cell attachment and proliferation. This gradient polymeric substrate exhibited significantly less water absorption compared to a collagen matrix control. When implanted in a rabbit dural defect model, the trilayer substrate exhibited greater cell proliferation and similar biocompatibility as the autologous fascial tissue control.

Electrospun scaffolds have been utilized as drug delivery vehicles to promote recruitment of endogenous cells *via* chemoattractant gradients. A tri-component scaffold consisting of rapidly degrading poly(ethylene oxide) (PEO) with collagenase, slower-degrading hyaluronic acid (HA) with platelet-derived growth factor-AB (PDGF-AB), and PCL was designed to enable direct cell migration for connective tissue repair.[88] Upon implantation into rat meniscus defects, tri-component scaffolds achieved significantly higher cellularity compared to scaffolds without collagenase or PDGF-AB. An electrospun PCL scaffold functionalized with hydroxyapatite *via* polydopamine particles (PCL-PDA-HA) was combined with substance P (SP) to promote endogenous stem cell mobilization toward bone defects.[89] The combination of PCL-PDA-HA and SP enhanced *in situ* bone formation compared to control groups lacking either compound.

Electrospun fibers of varying composition can be collected independently and stacked to create scaffolds with gradients in composition. For example, agarose-gelatin based scaffolds were fabricated with mid-layers of functionalized PCL fibers.[41] PCL fibers contained a dual gradient of chondroitin sulfate and bioactive glass to engineer GAG-enriched and

mineralized cartilage. Gradients in both structure and material can be created by changing the material in the syringe and the distance between the syringe needle and collector. Composition and fiber alignment gradients were created by harvesting fibers of HAp and poly(lactic-co-glycolic) acid (PLGA) on a collector with reciprocating rotation within 30°. [90] A fiber alignment gradient was also created by depositing fibers between two parallel aluminum disks. As the layer with aligned fibers became thicker, the electric field weakened, resulting in a more random alignment.[91] Furthermore, gradient scaffolds have been created by coating electrospun fibers after fabrication. Scaffolds possessing a gradient in mineralization were formed by linearly exposing regions of a scaffold to simulated body fluid (SBF) for increasing durations.[48] Mechanical testing of the scaffold revealed that the mechanical properties, namely the resulting gradient in stiffness, were adequate for tendon-to-bone models.[48a] When seeded with adipose stromal cells (ASCs), osteogenic markers were positively correlated with mineral content.[48b]

Bidirectional gradient electrospinning offers an alternative to simple stacking of materials to create gradient scaffolds. In this system, two solutions are simultaneously electrospun onto a collector at inversely proportional flow rates.[92] Syringe pumps can also be employed to mix together two solutions at inverse rates before being spun, resulting in the deposition of a single fiber that varies in composition over time.[93] Electrospinning has also been combined with methods such as braiding and thermally induced phase separation (TIPS) to prepare scaffolds with widely varying properties. For example, a triple-layered vascular scaffold was created by first electrospinning an inner layer composed of thermoplastic polyurethane (PU), followed by braiding a layer of silk, and then freeze drying a layer of PU for a porous outer layer.[94] The lumen diameter of the scaffold was 3.18 mm with an average thickness of 1.05 mm, and the burst pressure was ~23,000 mmHg, which is sufficient for vascular graft applications. Human umbilical vein endothelial cells formed a confluent layer on the inner surface of the scaffold with high cell viability. Therefore, electrospinning can produce FGMs in numerous ways and is highly compatible with other fabrication methods. It is inexpensive and scalable, enabling production of large quantities of scaffold with versatile gradients. However, the process is damaging to cells due to the use of cytotoxic solvents and possible shear-forces upon extrusion. Furthermore, extensive optimization is required for consistent production.

2.5 Freeze-drying

Freeze-drying, in which materials are frozen and ice crystals subsequently removed by sublimation, can yield several kinds of gradient materials.[95] Freeze-drying is an effective method to create a porous architecture in materials, in which the resulting pores are inverse images of the frozen solvent crystals.[96] Freeze-drying offers the ability to tailor a material's physical properties based on the solvents and solutes used.[96]

Iterative freeze-drying is an effective approach to bind multiple layers and create a gradient scaffold through interfacial adhesion, with scaffolds often used at the bone-cartilage or bone-tendon interface. For example, collagen-chitosan–polycaprolactone (CH–PCL) copolymer and chondroitin sulfate (CS) were mixed at various ratios to create a stratified scaffold for articular repair.[42] After each layer was created, the scaffold was freeze-dried to generate

both a porosity and composition gradient between layers. This technique has been used with multiple biomaterials for osteochondral defects including collagen,[97] alginate-chitosan β-TCP,[98] HAp/PVA,[99] and glycosaminoglycan-porous titanium[100]. Porosity gradients have been created in collagen *via* freeze-drying to test the effect of pore size on fibroblasts.[101] By varying collagen concentration from 0.26% to 0.13% prior to freeze-drying, pores were created ranging from ~87 μm to ~166 μm, demonstrating the relationship between protein concentration and resultant pore size as a design tool for fabricating gradient scaffolds.

Freeze-casting is a related process wherein a material is frozen to induce anisotropic formation of ice crystals that are then sublimated to create a porosity gradient. This process is commonly applied to ceramics such as biomimetic titanium alloys for dental and orthopaedic implants.[102] After freeze-casting, ceramics can be fired where they are exposed to high temperature and pressure, resulting in a material with a flexural strength in the hundreds of megapascals.[103] The resulting structure is dense at one end to support loading and becomes increasingly porous to promote bone growth. For example, HAp particles were freeze-casted around a frozen copper rod, resulting in expulsion of the HA particles and assembly into a lamellar structure oriented parallel to the freezing direction. [104] Due to the radial gradient of ice formation, the lamellar spacing becomes wider towards the outside and enables self-seeding of cells due to capillary action. Freeze-casting is amenable for combination with other techniques such as electrospinning[105] or solvent-casting to generate FGMs. It is a low-cost method for generation of porosity gradients. However, it is not amenable for concurrent seeding of cells.

2.6 Solvent casting and particulate leaching

Solvent casting and particulate leaching is a coordinated process used primarily for forming macroporous scaffolds that include randomly oriented pores.[106] This technique is also useful to form porosity or compositional gradients. Porogen particles (*e.g.*, salt, sugar, gelatin, *etc.*) are dispersed in a solvent which is allowed to evaporate, and the composite material is then placed in a bath to leach out the porogen (Figure 4A).[107] The simplest porosity gradient can be observed in bilayer scaffolds such as those used for osteochondral defects. Macroporous PLGA scaffolds were formed *via* particulate leaching with pore sizes ranging from 50 to 450 μm.[108] A mixture of PLGA and sodium chloride particulates was dissolved in dichloromethane and pressed into a mold, followed by porogen leaching in water. Multiple types of porogens can be used to create a gradient in pore size while preserving continuity between layers of a multilayered scaffold. A monolithic scaffold was created by first layering sucrose crystals and HA followed by mannitol crystals and PCL. [109] The sucrose and mannitol were removed by rinsing with water, resulting in a monolithic graft with varying pore size and composition.

Melt mixing and particulate leaching have been combined to make PCL,[110] PLA,[111] and PCL/PLA[112] gradient scaffolds. PCL and PLA were mixed at known ratios with PEG and NaCl and compressed, and PEG and NaCl were removed by particulate leaching in water. The PLA layer had pores ranging from 90 to 110 μm, while the PCL layer had pores ranging from 5 μm to 40 μm based on the size of NaCl used as the porogen. Solvent leaching was combined with TIPS to create a graded composite membrane.[113] PLGA solutions were

mixed with non-stoichiometric nanosized HAp (nano-HAp) and lauric acid (LA) in DMSO. Tri-layer scaffolds were then created by layering solutions with a graded composition of nano-HAp and LA and freezing the scaffold before the application of each subsequent layer. The frozen scaffold was submerged in water to remove the DMSO and create a composite graded scaffold. In another example, PLLA scaffolds possessing a porosity gradient were formed through TIPS by mixing sugar particles of decreasing diameter while applying heat. Scaffolds underwent phase separation overnight at −20°C with subsequent freeze-drying and particulate leaching.[114] The resulting scaffolds had a gradient in pore size from 300 to 600 μm, demonstrating the promise of this method to create scaffolds useful for tissue engineering (Figure 4B). Solvent casting and particulate leaching is an inexpensive method to form complex pore size and density gradients. Compared to freeze-casting, gradient formation is more precisely controlled, however the use of additional reagents is required for pore formation.

3. Application of functionally graded materials in model systems and engineered tissues

Native graded tissues are anisotropic in multiple properties including stiffness, composition, structure, and chemical concentration. When developing model systems, it is necessary to consider these factors to accurately recreate the stimuli to which cells are exposed. In light of the failure of uniform substrates lacking the presence of gradients, it is essential to engineer graded materials for producing more accurate model systems. The following section describes recent examples of model systems based on FGMs.

3.1 Musculoskeletal and connective tissues

The musculoskeletal system is a key target for the development of FGMs due to the number of native heterogeneous tissue interfaces. Bone, articular cartilage, tendon-to-bone, tendon-to-muscle, and ligament-to-bone interfaces exhibit complex architectural and compositional organization. Furthermore, many of these tissues are susceptible to injury at the interface due to the biomechanical differences between hard and soft tissues.[115] Therefore, the creation of FGMs to mimic these interfaces holds great potential for understanding and treating these injuries.

3.1.1 Enthesis models—The tendon- and ligament-to-bone interface (enthesis) is a common site of repair in patients of all ages with injuries such as tennis or golfer's elbow, jumper's knee, and Achilles insertional tendinopathies.[116] Depending on the severity of the injury, current treatment methods range from rest and steroid injections to surgical interventions and tissue grafts.[117] However, allogeneic grafts face several major shortcomings including host tissue reaction and risk of disease transmission, while autologous tissue grafting is limited by tissue availability and donor site morbidity.[118] Furthermore, grafts are associated with high injury recurrence rates due to formation of neofibrovascular tissue that compromises graft integrity.[118a, 119] The enthesis is divided into four distinct zones composed of varying cell types, matricellular proteins and proteoglycans, resulting in a tissue with a gradient in mechanical properties.[120] In light of the complexity of this tissue, there is a significant need to develop improved model systems

to understand the biophysical requirements of the enthesis and realize the goal of generating replacement tissue for these injuries.

Multi-layered scaffolds have been created as FGMs to mimic the structural, mechanical, and topographical properties of the bone-soft tissue interface. Synthetic polymers are often used including PCL, a common polymer used for bone tissue engineering due to its slow degradation, and PLGA for its application in modeling soft tissues and its absorbable nature. [121] Scaffolds for the bone-ligament interface possessing a gradient of physical and mechanical properties were fabricated by 3D printing a layer of PCL and then electrospinning PLGA on top. MSCs seeded on this gradient scaffold exhibited increased alkaline phosphatase activity and glycosaminoglycan production compared to MSCs on the individual scaffold components.[121] The instructive potential of fiber alignment within FGMs is under development to model and replace bone-patellar tendon-bone grafts, which are considered the gold standard for anterior cruciate ligament (ACL) ruptures.[122] Tissue engineered enthesis models were formulated with randomly aligned PLGA fibers that transitioned to aligned PCL and then back to randomly aligned PLGA to mimic the structural properties of bone-patellar tendon-bone grafts. A random-to-aligned scaffold of PCL for hard-soft tissue interfaces was seeded with osteosarcoma cells in the random region and fibroblasts in the aligned region.[123] Fibroblasts grew aligned along the fibers, while osteosarcoma cells maintained a random orientation. Both cell types migrated into the transition zone, providing a potential model for mimicking the transitional interface between bone and soft tissue. To complement the effect of gradients in fiber alignment, regions of PCL and PLGA scaffolds were soaked in SBF, resulting in a mineralized gradient that mimics the bone-ligament connection.[48b, 124] Hybrid scaffolds composed of ceramics and polymers such as β-TCP and poly(glycerol sebacate) (PGS) are also under investigation to model the bone-soft tissue interface.[125] PGS served as a barrier membrane when seeded with fibroblasts to combat scar formation with inferior mechanical properties.

While some FGMs seek to model the entire enthesis structure using synthetic polymers, others aim to recreate the collagen gradient present at the enthesis. Four-layered scaffolds were formed with a tendon layer composed of collagen, an uncalcified fibrocartilage layer of collagen and chondroitin sulfate, a calcified cartilage layer of collagen and low concentration apatite, and a bony layer composed of collagen and high concentration apatite. [97c] The scaffold supported the adhesion and proliferation of fibroblasts, chondrocytes, and osteoblasts toward each corresponding matrix. Salt leaching and freeze drying was used to create gradients in pore alignment from anisotropic to isotropic pore structure in order to mimic collagen alignment at the tendon/ligament-to-bone interface.[126] MSCs exhibited gradients in gene expression of tendon/ligament and cartilaginous markers along the scaffold in the absence of soluble factors, confirming the instructive potential of the substrate on cell differentiation. Collagen-GAG scaffolds incorporated both structural and biochemical cues consisting of coincident gradients of mineralization and geometric anisotropy present in native bone-tendon junctions.[49] The spatially graded contact and mineralization cues encouraged 3D alignment of tenocytes and selective pro-tenogenic and osteogenic MSC differentiation within a single scaffold. While these approaches expand our current understanding of enthesis function, the field currently lacks a standardized set of parameters for evaluation and use in the clinic. As a result, the results of mechanical and biochemical

tests are challenging to compare across studies or to native tissue. Furthermore, there is a lack of large animal studies to propel these technologies along the developmental timeline.

3.1.2   Osteochondral models—The ECM of articular cartilage varies from predominantly collagen type II in the superficial zone to increasing amounts of collage type X, proteoglycans, and sulfated glycosaminoglycans (sGAGs) in the deep zone with increasing mineralization.[7b, 115] Collagen fiber alignment is similar to that found in the enthesis, where collagen alignment is parallel at the articular surface and becomes increasingly perpendicular towards the subchondral surface.[127] Chondrocyte morphology also varies from thin and elliptical at the articular surface to more spherical chondrocytes oriented in stacks perpendicular to the articular surface.[127] This graded structure provides a smooth, lubricated surface for articulation and facilitates the transmission of loads with low friction.[128] In light of these gradients, FGMs are promising candidates to model the zonal structure found in articular cartilage.

The bone-cartilage interface is modeled with FGMs using similar approaches as used in models of the enthesis. Gradients in inductive cues (*i.e.*, growth factors) are under investigation to recapitulate osteochondral tissue. A chitosan-gelatin hydrogel/PLGA scaffold with dual-delivery of TGF-β1 and BMP-2 was designed to promote the differentiation of MSCs to chondrocytes and osteoblasts.[129] *In vitro* culture of MSCs confirmed that the hydrogel and PLGA phases promoted chondrogenic and osteogenic differentiation, respectively. This strategy also leverages the contributions of substrate stiffness to guide cell fate, with stiffer materials effectively inducing cells toward the osteogenic phenotype. When tested in rabbit osteochondral defects, the construct achieved successful integration of hyaline-like cartilage and mineralized tissue with native tissues at 2 months. Microfluidic platforms can be used to deliver gradients of osteogenic and chondrogenic inductive media to designated parts of a scaffold to create a similar gradient. [130] Microfluidics were combined with a bioreactor system to deliver various inductive media to form osteochondral constructs for studying osteoarthritis.[131] However, this method is ultimately limited to smaller constructs and lacks the native complexities associated with the development of osteoarthritis *in vivo*.

Osteochondral tissues can be modeled by the presentation of mineral gradients. Improved osteochondral tissue regeneration was observed with a bilayer scaffold of chitosan and HA as the cartilage layer and chitosan-alginate and HAp as the bone layer.[132] The cartilage region was defined by lower stiffness and the presence of HA, as found in native cartilage, while the bone layer was optimized for higher stiffness and osteoconductive HAp. Osteochondral tissue was modeled with an injectable, semi-interpenetrating network hydrogel construct containing chondroitin sulfate nanoparticles and nano-HAp in chondral and subchondral hydrogel zones, respectively.[133] The composite scaffold demonstrated accelerated osteochondral tissue generation in a rabbit osteochondral defect compared to monophasic and untreated controls (Figure 3C). Bilayer scaffolds consisting of a silk fibroin layer and a silk-CaP layer were implanted in a rabbit critically-sized osteochondral defect. [47] Developing tissues were positive for collagen type II and GAG within the silk layer, while *de novo* bone growth and capillary invasion were observed in the silk-CaP layer. Other

ceramics such as β-TCP are effective to introduce mineralization to osteochondral scaffolds and increase mechanical strength.[134]

Spatial gradients are also under examination to address damage to cartilage with healthy underlying bone. Anisotropic pore geometries were formed by unidirectional freeze-drying of alginate scaffolds that were further functionalized with collagen type I and II.[135] This strategy resulted in improved scaffold mechanical properties and promoted greater sGAG and collagen deposition compared to an isotropic pore geometry when seeded with human infrapatellar fat pad (IFP)-derived stromal cells. Freeze-drying was combined with centrifugation to create a porosity gradient in silk fibroin-chitosan-nano-HAp scaffolds.[136] Scaffolds with porosities ranging from 82–91% supported proliferation of MSCs. These studies suggest the promise of using porosity gradients to match the progressive osteochondral porosity structure observed in vivo. As discussed previously, stiffness is another key parameter that can be manipulated in model gradient systems. For example, gradients in stiffness ranging from 5–60 kPa were achieved by varying the concentration of PEG from 2–20% (w/v).[26b] Both chondrocytes and MSCs encapsulated in these gels with gradients in stiffness exhibited zonal specific responses and extracellular deposition that was abolished by blebbistatin, confirming the importance of mechanotransduction in the cell response to the stiffness gradient. FGMs are a promising advancement for the repair of osteochondral tissue due to its heterogeneous nature. Gradient scaffolds consistently outperform monophasic scaffolds in osteochondral defect models, illustrating the importance of recapitulating *in vivo* gradients for successful osteochondral repair.

3.2   Models of cancer

FGMs are widely applicable to cancer models given the array of signaling that occurs in the tumor microenvironment. Tumor cells are constantly remodeling surrounding tissues and changing the native physiological environment, resulting in gradients in soluble cues and stiffness that signal surrounding cells. *In vitro* models can improve the collective understanding of how biological gradients drive tumorigenesis and metastasis to assist in the development of improved treatments.

Haptotaxis, the migration of cells in response to a gradient of surface-bound molecules, is a predominant mechanism of signaling in cancer in which fibronectin (FN) concentration varies substantially throughout tumors.[137] Gradients of FN were formed in a microfluidic device to study the role of matricellular proteins on the migration of MDA-MB-231 breast adenocarcinoma cells. The results of this study identified a new haptotaxis mechanism, which is driven by the actin regulatory protein Mena that promotes ECM remodeling along FN gradients. Cells can also migrate in response to the alignment of ECM fibers. Specifically, MDA-MB-231 cells migrated faster on aligned collagen fibers compared to random, unaligned fibers.[138] The spacing of ECM fibers is yet another important consideration for cancer cell migration. FN-coated nanoscale posts were fabricated with a gradient in spacing from 0.3 to 4.2 μm.[139] When posts were coated with 10 μg mL^{-1} of FN, invasive 1205Lu melanoma cells accumulated in areas of sparser spacing, while cells accumulated in denser arrays at 50 μg mL^{-1} FN due to the balance of ECM-triggered signaling pathways PI(3)K–Akt and ROCK–MLCK. Breast cancer (MDA-MB-231),

fibrosarcoma (HT1080), and glioblastoma (T98G) cells on a PA gel with a gradient in stiffness from 2 to 20 kPa underwent durotaxis, exhibiting biased migration towards the stiffer regions.[140] Human cancer cells of varying tissue origins also exhibit durotaxis from soft to stiff regions of a substrate.[140]

Some cancer models include an oxygen gradient to mimic hypoxia, which is a critical factor in the progression and metastasis of many cancers. Primary mouse sarcoma cells were encapsulated in oxygen (O_2)-controllable hydrogels which recreated pathophysiological O_2 levels *in vitro*.[141] Compared to control gels, cell invasion was faster and extended over longer distances in the direction of increasing O_2 tension in gels with oxygen gradients. Overall, FGMs can further elucidate mechanisms behind cancer cell migration and metastasis. The precise control of microfluidics makes them a common choice for modeling the cancer cell environment and examining cell response to individual parameters such as protein concentration or oxygen tension.

3.3 Drug screening platforms

FGMs are useful in diagnostic devices due to their ability to subject cells to a wide range of conditions, identify effective and cytotoxic concentrations of drugs, or determine how cells interact with ECM conditions. A high throughput drug system was developed using combinatorial concentrations of drugs generated by two microfluidic mixers, resulting in 64 unique combinations.[142] The efficacy of chemotherapeutics on prostate cancer was then investigated by applying these combinations to human PC3 prostate cells while minimizing the volume of required reagents. Microfluidic devices can also be constructed to replicate *in vivo* environments of tumor cells to more accurately assess the dose-response effect of cells exposed to drugs. The chemotherapeutic effect of various drugs was studied in a colorectal tumor-on-a-chip system consisting of a central chamber surrounded by a pair of perfusable channels. By generating a gradient of chemotherapeutic drug, the platform established a dose-dependent response of exposed cells and enabled analysis of gene expression to identify new druggable targets. The hypoxia-dependent cytotoxicity of anticancer drugs has been investigated using microfluidic systems that enable the generation of reproducible oxygen gradients.[143] Adenocarcinoma (A549) cells cultured in this device were treated with tirapazamine (TPZ) under various oxygen tensions. These studies revealed the improved potency of TPZ under hypoxia compared to established chemotherapeutic agents such as cisplatin.[144] Gradients of ECM can be utilized to examine cell response *in vitro*. A three-dimensional array of ECM gradients was bioprinted by controlling the ratio of a GelMA hydrogel, which contains native adhesion ligands, to a PEGDA hydrogel, which is bioinert and lacks endogenous adhesion motifs.[145] The resulting array was used to screen the response of human periodontal ligament stem cells to the varying ECM content, with cell viability and spreading decreasing with increasing ratios of PEG. These platforms have the potential to advance personalized medicine, identify new potent drugs, and reduce healthcare expenses.

4. Conclusion and Future Outlook

FGMs are designed to replicate the heterogeneity of native tissues. If properly fabricated, FGMs could mimic the function of biological gradients such as mechanical support, presentation of instructive stimuli, application of physiologically relevant forces, and cell signaling. FGMs are created using a variety of techniques including light-based methods, 3D printing, microfluidics, and electrospinning. As discussed in this review, functional gradients have been utilized to create model systems such as bone-soft tissue interfaces that advance our understanding of physiology and pathology occurring at these interfacial tissues. Continued development of FGMs will expand their use to additional tissues such as nervous, cardiac, and dermal tissue that exhibit gradients in cell type, electroconductivity, and structure. Currently, many FGMs are engineered with linear gradients, yet gradients *in vivo* are often discontinuous or nonlinear. Cell differentiation, migration, and growth depend on nonlinear gradients that should be implemented in scaffolds to better mimic native conditions.[66] Upon implantation *in vivo*, FGMs may be subjected to external stimuli such as gradients in load. Many models of interfacial tissue do not presently consider the role of gradients in mechanical loading despite studies confirming cellular mechanosensitivity to loading.[146] The inclusion of nonlinear gradients will increase the efficacy of FGMs.

At this time, the majority of studies using functional gradients focus on spatial distribution of some characteristic including composition, stiffness, inductive factor, among others. These parameters are often established *a priori*, providing limited opportunities for the gradients to evolve in response to cells. It is imperative to incorporate more dynamic, temporally dependent aspects into FGMs to mimic native processes such as gene expression and evolving biochemical signals during cell differentiation. Technologies such as slow-releasing nanoparticle delivery systems and cell-responsive hydrogels could regulate the evolution of gradients in a more natural, temporal manner.[147]

The efficacy of FGMs as model systems is dependent upon ease of fabrication, simplicity of use, and reproducibility in resulting data. For these FGMs to be widely available, the methods employed must be simple and should be high throughput in nature to ensure translation to the clinic. Microfluidic platforms meet these requirements due to their consistent fabrication methods and minimal required reagent volume. However, in order to maintain their ease-of-use, microfluidics sacrifice the complexity present in many native tissues. While they are appropriate for studying basic cell interactions such as durotaxis or haptotaxis, more complex models are needed to accurately model native gradients *in vitro*.

The successful translation of FGMs to the clinic must overcome several challenges. Standardized manufacturing approaches are required to improve reproducibility and enable broad adoption. In accordance with standardization techniques, improved strategies for quality assurance will ensure consistent gradient formation. Compared to homogeneous materials that exhibit predictable changes in biophysical properties, heterogeneous constructs have a range of values that must be verified, necessitating the development of improved technologies to characterize FGMs directly. The scale-up of constructs for large injuries that occur in the body represents another major challenge in the translation of FGMs to human patients. Large constructs require sufficient nutrient transport to enable survival of

transplanted or invading cells. The combination of technologies such as 3D printing and electrospinning may facilitate the scaling up of constructs with graded components such as porosity and peptide concentration to promote vascularization. Tissue substitutes must also be customized to fit the defect sites of patients. The advancement of 3D printing combined with imaging modalities such as computed tomography (CT) may enable rapid prototyping of customized FGMs and increase their use in the clinic. By addressing these challenges, FGMs will provide a valuable tool for understanding and repairing heterogeneous tissues found in the body.

Acknowledgements

Author Profiles

Jeremy Lowen is a Ph.D. student in biomedical engineering at the University of California, Davis. After obtaining his undergraduate degree in biomedical engineering, he started his graduate work with Dr. Kent Leach. His research interests include creating functional materials for osteochondral regeneration and translational applications of microfluidics.

Dr. Kent Leach is a Professor of Biomedical Engineering and Orthopaedic Surgery at the University of California, Davis. His laboratory is interested in the design and utilization of instructive biomaterials to direct cell fate. His work is highly translational, and his lab works closely with a number of clinical partners in Orthopaedic Surgery at UC Davis Health and the UC Davis School of Veterinary Medicine to translate the findings to the clinic.

References

[1]. (a)Miyamoto Y, Kaysser WA, Rabin BH, Kawasaki A, Ford RG, Functionally Graded Materials: Design, Processing and Applications, Springer US, 2013;(b)Koizumi M, Niino M, MRS Bulletin 2013, 20, 19.

[2]. (a)Gong T, Xie J, Liao J, Zhang T, Lin S, Lin Y, Bone Res. 2015, 3, 15029; [PubMed: 26558141] (b)Pompe W, Worch H, Epple M, Friess W, Gelinsky M, Greil P, Hempel U, Scharnweber D, Schulte K, Mat Sci Eng a-Struct 2003, 362, 40.

[3]. (a)Genin GM, Kent A, Birman V, Wopenka B, Pasteris JD, Marquez PJ, Thomopoulos S, Biophys. J 2009, 97, 976; [PubMed: 19686644] (b)Qu J, Thoreson AR, Chen Q, An KN, Amadio PC, Zhao C, J. Orthop. Res 2013, 31, 1713. [PubMed: 23939935]

[4]. Kwon H, Brown WE, Lee CA, Wang D, Paschos N, Hu JC, Athanasiou KA, Nat. Rev. Rheumatol 2019, 15, 550. [PubMed: 31296933]

[5]. Wu J, Mao Z, Tan H, Han L, Ren T, Gao C, Interface Focus 2012, 2, 337. [PubMed: 23741610]

[6]. Li J, Mooney DJ, Nat. Rev. Mater 2016, 1, 16071. [PubMed: 29657852]

[7]. (a)Chai Q, Jiao Y, Yu X, Gels 2017, 3;(b)Gadjanski I, F1000Res. 2017, 6.

[8]. Yahia L, J. Biomed. Sci 2015, 04.

[9]. Madou MJ, Fundamentals of Microfabrication: The Science of Miniaturization, Second Edition, Taylor & Francis, 2002.

[10]. Jain G, Ford AJ, Rajagopalan P, ACS Biomater. Sci. Eng 2015, 1, 621. [PubMed: 33435085]

[11]. Tse JR, Engler AJ, PLoS One 2011, 6, e15978. [PubMed: 21246050]

[12]. Major LG, Holle AW, Young JL, Hepburn MS, Jeong K, Chin IL, Sanderson RW, Jeong JH, Aman ZM, Kennedy BF, Hwang Y, Han DW, Park HW, Guan KL, Spatz JP, Choi YS, ACS Appl. Mater. Interfaces 2019, 11, 45520. [PubMed: 31714734]

[13]. Hadden WJ, Young JL, Holle AW, McFetridge ML, Kim DY, Wijesinghe P, Taylor-Weiner H, Wen JH, Lee AR, Bieback K, Vo BN, Sampson DD, Kennedy BF, Spatz JP, Engler AJ, Choi YS, Proc. Natl. Acad. Sci. U. S. A 2017, 114, 5647. [PubMed: 28507138]

[14]. Kloxin AM, Benton JA, Anseth KS, Biomaterials 2010, 31, 1. [PubMed: 19788947]

[15]. Marklein RA, Burdick JA, Soft Matter 2010, 6, 136.

[16]. Sunyer R, Jin AJ, Nossal R, Sackett DL, PLoS One 2012, 7, e46107. [PubMed: 23056241]

[17]. Kloxin AM, Kasko AM, Salinas CN, Anseth KS, Science 2009, 324, 59. [PubMed: 19342581]

[18]. (a)Corum LE, Hlady V, Biomaterials 2010, 31, 3148; [PubMed: 20149436] (b)Ding YX, Streitmatter S, Wright BE, Hlady V, Langmuir 2010, 26, 12140. [PubMed: 20568822]

[19]. Norris SCP, Tseng P, Kasko AM, ACS Biomater. Sci. Eng 2016, 2, 1309. [PubMed: 33434984]

[20]. Horn-Ranney EL, Curley JL, Catig GC, Huval RM, Moore MJ, Biomed. Microdevices 2013, 15, 49. [PubMed: 22903647]

[21]. Denk W, Strickler JH, Webb WW, Science 1990, 248, 73. [PubMed: 2321027]

[22]. Tam RY, Smith LJ, Shoichet MS, Acc. Chem. Res 2017, 50, 703. [PubMed: 28345876]

[23]. Aizawa Y, Shoichet MS, Biomaterials 2012, 33, 5198. [PubMed: 22560669]

[24]. (a)DeLong SA, Gobin AS, West JL, J. Control. Release 2005, 109, 139; [PubMed: 16290119] (b)Yang YH, Khan Z, Ma C, Lim HJ, Smith Callahan LA, Acta Biomater. 2015, 21, 55. [PubMed: 25931018]

[25]. (a)Hill MC, Nguyen MK, Jeon O, Alsberg E, Adv. Healthc. Mater 2015, 4, 714; [PubMed: 25530099] (b)Jeon O, Alt DS, Linderman SW, Alsberg E, Adv. Mater 2013, 25, 6366. [PubMed: 23983019]

[26]. (a)Lim HJ, Khan Z, Wilems TS, Lu X, Perera TH, Kurosu YE, Ravivarapu KT, Mosley MC, Callahan LAS, ACS Biomater. Sci. Eng 2017, 3, 776; [PubMed: 33440502] (b)Zhu D, Tong X, Trinh P, Yang F, Tissue Eng., Part A 2018, 24, 1. [PubMed: 28385124]

[27]. Larsen EKU, Larsen NB, Almdal K, Larsen EKU, Larsen NB, Almdal K, J Polym Sci Pol Phys 2016, 54, 1195.

[28]. Bailey BM, Nail LN, Grunlan MA, Acta Biomater. 2013, 9, 8254. [PubMed: 23707502]

[29]. Ko H, Suthiwanich K, Mary H, Zanganeh S, Hu SK, Ahadian S, Yang Y, Choi G, Fetah K, Niu Y, Mao JJ, Khademhosseini A, Biofabrication 2019, 11, 025014. [PubMed: 30786263]

[30]. Zorlutuna P, Annabi N, Camci-Unal G, Nikkhah M, Cha JM, Nichol JW, Manbachi A, Bae H, Chen S, Khademhosseini A, Adv. Mater 2012, 24, 1782. [PubMed: 22410857]

[31]. Nguyen TU, Watkins KE, Kishore V, J. Biomed. Mater. Res., Part A 2019, 107, 1541.

[32]. Khorshidi S, Karkhaneh A, J. Tissue Eng. Regen. Med 2018, 12, e1974. [PubMed: 29243352]

[33]. Knowlton S, Anand S, Shah T, Tasoglu S, Trends Neurosci. 2018, 41, 31. [PubMed: 29223312]

[34]. Bouthillier JL, Carbon3D – Terminator Inspired 3D Printing Technology, http://bootsindustries.com/carbon3d-terminator-inspired-3d-printing-technology/, accessed: 18.10.2019.

[35]. Hinton TJ, Jallerat Q, Palchesko RN, Park JH, Grodzicki MS, Shue HJ, Ramadan MH, Hudson AR, Feinberg AW, Sci. Adv 2015, 1, e1500758. [PubMed: 26601312]

[36]. Scaffaro R, Lopresti F, Maio A, Sutera F, Botta L, J. Appl. Biomater. Funct. Mater 2017, 15, e107. [PubMed: 28009418]

[37]. Kim SE, Harker EC, De Leon AC, Advincula RC, Pokorski JK, Biomacromolecules 2015, 16, 860. [PubMed: 25715836]

[38]. Di Luca A, Longoni A, Criscenti G, Lorenzo-Moldero I, Klein-Gunnewiek M, Vancso J, van Blitterswijk C, Mota C, Moroni L, Biofabrication 2016, 8, 015014. [PubMed: 26924824]

[39]. Lee CH, Rodeo SA, Fortier LA, Lu C, Erisken C, Mao JJ, Sci. Transl. Med 2014, 6, 266ra171.

[40]. D'Amora U, D'Este M, Eglin D, Safari F, Sprecher CM, Gloria A, De Santis R, Alini M, Ambrosio L, J. Tissue Eng. Regen. Med 2018, 12, 321. [PubMed: 28486746]

[41]. Mohan N, Wilson J, Joseph D, Vaikkath D, Nair PD, J. Biomed. Mater. Res., Part A 2015, 103, 3896.

[42]. Zhu Y, Wu H, Sun S, Zhou T, Wu J, Wan Y, J. Mech. Behav. Biomed. Mater 2014, 36, 32. [PubMed: 24793172]

[43]. Wang YF, Guo HF, Ying DJ, J. Biomed. Mater. Res., Part B 2013, 101, 1359.

[44]. Bittner SM, Smith BT, Diaz-Gomez L, Hudgins CD, Melchiorri AJ, Scott DW, Fisher JP, Mikos AG, Acta Biomater. 2019, 90, 37. [PubMed: 30905862]

[45]. Gonzalez-Fernandez T, Rathan S, Hobbs C, Pitacco P, Freeman FE, Cunniffe GM, Dunne NJ, McCarthy HO, Nicolosi V, O'Brien FJ, Kelly DJ, J. Control. Release 2019, 301, 13. [PubMed: 30853527]

[46]. Gao F, Xu ZY, Liang QF, Liu B, Li HF, Wu YH, Zhang YY, Lin ZF, Wu MM, Ruan CS, Liu WG, Adv. Funct. Mater 2018, 28.

[47]. Yan LP, Silva-Correia J, Oliveira MB, Vilela C, Pereira H, Sousa RA, Mano JF, Oliveira AL, Oliveira JM, Reis RL, Acta Biomater. 2015, 12, 227. [PubMed: 25449920]

[48]. (a)Lipner J, Liu W, Liu Y, Boyle J, Genin GM, Xia Y, Thomopoulos S, J. Mech. Behav. Biomed. Mater 2014, 40, 59; [PubMed: 25194525] (b)Liu W, Lipner J, Xie J, Manning CN, Thomopoulos S, Xia Y, ACS Appl. Mater. Interfaces 2014, 6, 2842. [PubMed: 24433042]

[49]. Caliari SR, Weisgerber DW, W. K., Mahmassani Z, Boppart MD, Harley BA, Adv. Healthc. Mater 2015, 4, 831. [PubMed: 25597299]

[50]. Rhee S, Puetzer JL, Mason BN, Reinhart-King CA, Bonassar LJ, ACS Biomater. Sci. Eng 2016, 2, 1800. [PubMed: 33440478]

[51]. Ren X, Wang F, Chen C, Gong X, Yin L, Yang L, BMC Musculoskelet. Disord 2016, 17, 301. [PubMed: 27439428]

[52]. Lee KY, Mooney DJ, Prog. Polym. Sci 2012, 37, 106. [PubMed: 22125349]

[53]. Sultan S, Mathew AP, Nanoscale 2018, 10, 4421. [PubMed: 29451572]

[54]. Petit C, Montanaro L, Palmero P, Int. J. Appl. Ceram 2018, 15, 820.

[55]. Liu J, Li L, Suo H, Yan M, Yin J, Fu J, Mater. Des 2019, 171.

[56]. Jones JR, Acta Biomater. 2013, 9, 4457. [PubMed: 22922331]

[57]. Gao F, Xu Z, Liang Q, Li H, Peng L, Wu M, Zhao X, Cui X, Ruan C, Liu W, Adv. Sci 2019, 6, 1900867.

[58]. Gingter P, Watjen AM, Kramer M, Telle R, J. Ceram. Sci. Technol 2015, 6, 119.

[59]. Phillippi JA, Miller E, Weiss L, Huard J, Waggoner A, Campbell P, Stem Cells 2008, 26, 127. [PubMed: 17901398]

[60]. Miller ED, Phillippi JA, Fisher GW, Campbell PG, Walker LM, Weiss LE, Comb. Chem. High Throughput Screening 2009, 12, 604.

[61]. Hubka KM, Carson DD, Harrington DA, Farach-Carson MC, Acta Biomater. 2019, 97, 385. [PubMed: 31351252]

[62]. Mandrycky C, Wang Z, Kim K, Kim DH, Biotechnol. Adv 2016, 34, 422. [PubMed: 26724184]

[63]. Wang X, Liu ZM, Pang Y, Rsc Adv 2017, 7, 29966.

[64]. Chen C, Mehl BT, Munshi AS, Townsend AD, Spence DM, Martin RS, Anal. Methods 2016, 8, 6005. [PubMed: 27617038]

[65]. Uzel SG, Amadi OC, Pearl TM, Lee RT, So PT, Kamm RD, Small 2016, 12, 612. [PubMed: 26619365]

[66]. Selimovic S, Sim WY, Kim SB, Jang YH, Lee WG, Khabiry M, Bae H, Jambovane S, Hong JW, Khademhosseini A, Anal. Chem 2011, 83, 2020. [PubMed: 21344866]

[67]. Shi X, Zhou J, Zhao Y, Li L, Wu H, Adv. Healthc. Mater 2013, 2, 846. [PubMed: 23193109]

[68]. Wertheim L, Shapira A, Amir RJ, Dvir T, Nanotechnology 2018, 29, 13LT01.

[69]. Morrow CM, Mukherjee A, Traore MA, Leaman EJ, Kim A, Smith EM, Nain AS, Behkam B, Lab Chip 2019, 19, 3641. [PubMed: 31560021]

[70]. Garcia S, Sunyer R, Olivares A, Noailly J, Atencia J, Trepat X, Lab Chip 2015, 15, 2606. [PubMed: 25977997]

[71]. Hsieh HY, Camci-Unal G, Huang TW, Liao R, Chen TJ, Paul A, Tseng FG, Khademhosseini A, Lab Chip 2014, 14, 482. [PubMed: 24253194]

[72]. Bazban-Shotorbani S, Dashtimoghadam E, Karkhaneh A, Hasani-Sadrabadi MM, Jacob KI, Langmuir 2016, 32, 4996. [PubMed: 26938744]

[73]. Xin S, Dai J, Gregory CA, Han A, Alge DL, Adv. Funct. Mater 2019, DOI: 10.1002/adfm.201907102.

[74]. Tonon F, Giobbe GG, Zambon A, Luni C, Gagliano O, Floreani A, Grassi G, Elvassore N, Sci. Rep 2019, 9, 13557. [PubMed: 31537830]

[75]. Lam SF, Shirure VS, Chu YE, Soetikno AG, George SC, PLoS One 2018, 13, e0209574. [PubMed: 30571786]

[76]. Liu ZZ, Sun H, Ren KN, Chempluschem 2017, 82, 792. [PubMed: 31961536]

[77]. Carvalho MR, Barata D, Teixeira LM, Giselbrecht S, Reis RL, Oliveira JM, Truckenmuller R, Habibovic P, Sci. Adv 2019, 5, eaaw1317.

[78]. Zhang F, Tian C, Liu W, Wang K, Wei Y, Wang H, Wang J, Liu S, ACS Sens. 2018, 3, 2716. [PubMed: 30507116]

[79]. Sundararaghavan HG, Masand SN, Shreiber DI, J. Neurotrauma 2011, 28, 2377. [PubMed: 21473683]

[80]. Movilla N, Borau C, Valero C, Garcia-Aznar JM, Bone 2018, 107, 10. [PubMed: 29107125]

[81]. Lin FY, Lin JY, Lo KY, Sun YS, Int. J. Mol. Sci 2019, 20.

[82]. Costantini M, Jaroszewicz J, Kozon L, Szlazak K, Swieszkowski W, Garstecki P, Stubenrauch C, Barbetta A, Guzowski J, Angew. Chem. Int. Ed. Engl 2019, 58, 7620. [PubMed: 30908850]

[83]. Zhang X, Gao X, Jiang L, Qin J, Langmuir 2012, 28, 10026. [PubMed: 22607039]

[84]. Xue J, Xie J, Liu W, Xia Y, Acc. Chem. Res 2017, 50, 1976. [PubMed: 28777535]

[85]. Ingavle GC, Leach JK, Tissue Eng., Part B 2014, 20, 277.

[86]. Braghirolli DI, Steffens D, Pranke P, Drug Discov. Today 2014, 19, 743. [PubMed: 24704459]

[87]. Bye FJ, Bissoli J, Black L, Bullock AJ, Puwanun S, Moharamzadeh K, Reilly GC, Ryan AJ, MacNeil S, Biomater Sci-Uk 2013, 1, 942.

[88]. Qu F, Holloway JL, Esterhai JL, Burdick JA, Mauck RL, Nat. Commun 2017, 8, 1780. [PubMed: 29176654]

[89]. Lee JS, Jin Y, Park HJ, Yang K, Lee MS, Yang HS, Cho SW, Biotechnol. J 2017, 12.

[90]. He JK, Qin T, Liu YX, Li X, Li DC, Jin ZM, Mater Lett 2014, 137, 393.

[91]. (a)Pu J, Komvopoulos K, Acta Biomater. 2014, 10, 2718; [PubMed: 24434536] (b)Pu J, Yuan F, Li S, Komvopoulos K, Acta Biomater. 2015, 13, 131. [PubMed: 25463495]

[92]. (a)Wu T, Huang C, Li D, Yin A, Liu W, Wang J, Chen J, Ei-Hamshary H, Al-Deyab SS, Mo X, Colloids Surf. B Biointerfaces 2015, 133, 179; [PubMed: 26101818] (b)Yang G, Lin H, Rothrauff BB, Yu S, Tuan RS, Acta Biomater. 2016, 35, 68. [PubMed: 26945631]

[93]. A. P., Robbins AB, Mohiuddin SF, Jiang M, Moreno MR, Cosgriff-Hernandez EM, Acta Biomater. 2017, 56, 118. [PubMed: 28017867]

[94]. Mi H-Y, Jing X, Yu E, McNulty J, Peng X-F, Turng L-S, Mater Lett 2015, 161, 305.

[95]. Morais AR, Alencar Edo N, Xavier Junior FH, de Oliveira CM, Marcelino HR, Barratt G, Fessi H, do Egito ES, Elaissari A, Int. J. Pharm 2016, 503, 102. [PubMed: 26943974]

[96]. Deville S, Materials 2010, 3, 1913.

[97]. (a)Levingstone TJ, Matsiko A, Dickson GR, O'Brien FJ, Gleeson JP, Acta Biomater. 2014, 10, 1996; [PubMed: 24418437] (b)Levingstone TJ, Ramesh A, Brady RT, Brama PAJ, Kearney C, Gleeson JP, O'Brien FJ, Biomaterials 2016, 87, 69; [PubMed: 26901430] (c)Kim BS, Kim EJ, Choi JS, Jeong JH, Jo CH, Cho YW, J. Biomed. Mater. Res., Part A 2014, 102, 4044.

[98]. Algul D, Sipahi H, Aydin A, Kelleci F, Ozdatli S, Yener FG, Int. J. Biol. Macromol 2015, 79, 363. [PubMed: 25982954]

[99]. Yusong P, Qianqian S, Chengling P, Jing W, J. Biomed. Mater. Res., Part B 2013, 101, 729.

[100]. Duan X, Zhu X, Dong X, Yang J, Huang F, Cen S, Leung F, Fan H, Xiang Z, Mater. Sci. Eng., C 2013, 33, 3951.

[101]. Wang Y, Xu R, Luo G, Lei Q, Shu Q, Yao Z, Li H, Zhou J, Tan J, Yang S, Zhan R, He W, Wu J, Acta Biomater. 2016, 30, 246. [PubMed: 26602823]

[102]. Zhang L, Le Coz-Botrel R, Beddoes C, Sjostrom T, Su B, Biomed. Mater 2017, 12, 015014. [PubMed: 28094241]

[103]. Hou Z, Ye F, Liu Q, Liu L, Jiang H, Zhang S, Materials 2019, 12.

[104]. Bai H, Wang D, Delattre B, Gao W, De Coninck J, Li S, Tomsia AP, Acta Biomater. 2015, 20, 113. [PubMed: 25871536]

[105]. Zhang S, Chen L, Jiang Y, Cai Y, Xu G, Tong T, Zhang W, Wang L, Ji J, Shi P, Ouyang HW, Acta Biomater. 2013, 9, 7236. [PubMed: 23567945]

[106]. Harris LD, Kim BS, Mooney DJ, J. Biomed. Mater. Res 1998, 42, 396. [PubMed: 9788501]

[107]. Prasad A, Sankar MR, Katiyar V, Mater Today-Proc 2017, 4, 898.

[108]. Duan P, Pan Z, Cao L, He Y, Wang H, Qu Z, Dong J, Ding J, J. Biomed. Mater. Res., Part A 2014, 102, 180.

[109]. Giannoni P, Lazzarini E, Ceseracciu L, Barone AC, Quarto R, Scaglione S, J. Tissue Eng. Regen. Med 2015, 9, 1182. [PubMed: 23172816]

[110]. Scaffaro R, Lopresti F, Botta L, Rigogliuso S, Ghersi G, Macromol Mater Eng 2016, 301, 182.

[111]. Scaffaro R, Lopresti F, Botta L, Rigogliuso S, Ghersi G, J. Mech. Behav. Biomed. Mater 2016, 54, 8. [PubMed: 26410761]

[112]. Scaffaro R, Lopresti F, Botta L, Rigogliuso S, Ghersi G, J. Mech. Behav. Biomed. Mater 2016, 63, 303. [PubMed: 27442921]

[113]. Jamuna-Thevi K, Saarani NN, Abdul Kadir MR, Hermawan H, Mater. Sci. Eng., C 2014, 43, 253.

[114]. Nie TT, Xue L, Ge M, Ma HY, Zhang JC, Mater Lett 2016, 176, 25.

[115]. Bayrak E, Huri PY, Front Mater 2018, 5.

[116]. (a)Benjamin M, Toumi H, Ralphs JR, Bydder G, Best TM, Milz S, J. Anat 2006, 208, 471; [PubMed: 16637873] (b)Benjamin M, Kumai T, Milz S, Boszczyk BM, Boszczyk AA, Ralphs JR, Comp. Biochem. Physiol., Part A: Mol. Integr. Physiol 2002, 133, 931;(c)Yamamoto A, Takagishi K, Osawa T, Yanagawa T, Nakajima D, Shitara H, Kobayashi T, J. Shoulder Elbow Surg 2010, 19, 116. [PubMed: 19540777]

[117]. Calejo I, Costa-Almeida R, Reis RL, Gomes ME, Tissue Eng.. Part B 2019, 25, 330.

[118]. (a)Kaeding CC, Aros B, Pedroza A, Pifel E, Amendola A, Andrish JT, Dunn WR, Marx RG, McCarty EC, Parker RD, Wright RW, Spindler KP, Sports Health 2011, 3, 73; [PubMed: 23015994] (b)Robertson A, Nutton RW, Keating JF, J. Bone Joint Surg. Br 2006, 88, 988. [PubMed: 16877593]

[119]. Lui P, Zhang P, Chan K, Qin L, J. Orthop. Surg. Res 2010, 5, 59. [PubMed: 20727196]

[120]. (a)Apostolakos J, Durant TJ, Dwyer CR, Russell RP, Weinreb JH, Alaee F, Beitzel K, McCarthy MB, Cote MP, Mazzocca AD, Muscles Ligaments Tendons J 2014, 4, 333; [PubMed: 25489552] (b)Font Tellado S, Balmayor ER, Van Griensven M, Adv. Drug Deliv. Rev 2015, 94, 126. [PubMed: 25777059]

[121]. Criscenti G, Longoni A, Di Luca A, De Maria C, van Blitterswijk CA, Vozzi G, Moroni L, Biofabrication 2016, 8, 015009. [PubMed: 26824799]

[122]. Samavedi S, Vaidya P, Gaddam P, Whittington AR, Goldstein AS, Biotechnol. Bioeng 2014, 111, 2549. [PubMed: 24898875]

[123]. Nowlin J, Bismi MA, Delpech B, Dumas P, Zhou Y, Tan GZ, Nanobiomedicine 2018, 5, 1849543518803538.

[124]. Lin ZF, Zhao XJ, Chen S, Du C, J Mater Chem B 2017, 5, 1015. [PubMed: 32263880]

[125]. Tevlek A, Hosseinian P, Ogutcu C, Turk M, Aydin HM, Mater. Sci. Eng., C 2017, 72, 316.

[126]. Font Tellado S, Bonani W, Balmayor ER, Foehr P, Motta A, Migliaresi C, van Griensven M, Tissue Eng., Part A 2017, 23, 859. [PubMed: 28330431]

[127]. Boushell MK, Hung CT, Hunziker EB, Strauss EJ, Lu HH, Connect. Tissue. Res 2017, 58, 393. [PubMed: 27599801]

[128]. Sophia Fox AJ, Bedi A, Rodeo SA, Sports Health 2009, 1, 461. [PubMed: 23015907]

[129]. Han F, Zhou F, Yang X, Zhao J, Zhao Y, Yuan X, J. Biomed. Mater. Res., Part B 2015, 103, 1344.

[130]. Goldman SM, Barabino GA, Biores. Open. Access 2016, 5, 109. [PubMed: 27190700]

[131]. Lin H, Lozito TP, Alexander PG, Gottardi R, Tuan RS, Mol. Pharm 2014, 11, 2203. [PubMed: 24830762]

[132]. Erickson AE, Sun J, Lan Levengood SK, Swanson S, Chang FC, Tsao CT, Zhang M, Biomed. Microdevices 2019, 21, 34. [PubMed: 30906951]

[133]. Radhakrishnan J, Manigandan A, Chinnaswamy P, Subramanian A, Sethuraman S, Biomaterials 2018, 162, 82. [PubMed: 29438883]

[134]. Li Z, Jia S, Xiong Z, Long Q, Yan S, Hao F, Liu J, Yuan Z, J. Biosci. Bioeng 2018, 126, 389. [PubMed: 29685821]

[135]. Almeida HV, Sathy BN, Dudurych I, Buckley CT, O'Brien FJ, Kelly DJ, Tissue Eng., Part A 2017, 23, 55. [PubMed: 27712409]

[136]. Xiao H, Huang W, Xiong K, Ruan S, Yuan C, Mo G, Tian R, Zhou S, She R, Ye P, Liu B, Deng J, Int. J. Nanomed 2019, 14, 2011.

[137]. Oudin MJ, Jonas O, Kosciuk T, Broye LC, Guido BC, Wyckoff J, Riquelme D, Lamar JM, Asokan SB, Whittaker C, Ma D, Langer R, Cima MJ, Wisinski KB, Hynes RO, Lauffenburger DA, Keely PJ, Bear JE, Gertler FB, Cancer Discov. 2016, 6, 516. [PubMed: 26811325]

[138]. Carey SP, Goldblatt ZE, Martin KE, Romero B, Williams RM, Reinhart-King CA, Integr. Biol 2016, 8, 821.

[139]. Park J, Kim DH, Kim HN, Wang CJ, Kwak MK, Hur E, Suh KY, An SS, Levchenko A, Nat. Mater 2016, 15, 792. [PubMed: 26974411]

[140]. DuChez BJ, Doyle AD, Dimitriadis EK, Yamada KM, Biophys. J 2019, 116, 670. [PubMed: 30709621]

[141]. Lewis DM, Park KM, Tang V, Xu Y, Pak K, Eisinger-Mathason TS, Simon MC, Gerecht S, Proc. Natl. Acad. Sci. U. S. A 2016, 113, 9292. [PubMed: 27486245]

[142]. An D, Kim K, Kim J, Biomol. Ther 2014, 22, 355.

[143]. Wang ZH, Liu ZX, Li LL, Liang QL, Microfluid Nanofluid 2015, 19, 1271.

[144]. Mulholland T, McAllister M, Patek S, Flint D, Underwood M, Sim A, Edwards J, Zagnoni M, Sci. Rep 2018, 8, 14672. [PubMed: 30279484]

[145]. Ma Y, Ji Y, Huang G, Ling K, Zhang X, Xu F, Biofabrication 2015, 7, 044105. [PubMed: 26696269]

[146]. Delaine-Smith RM, Reilly GC, Vitam. Horm 2011, 87, 417. [PubMed: 22127254]

[147]. (a)Kolachala VL, Henriquez OA, Shams S, Golub JS, Kim YT, Laroui H, Torres-Gonzalez E, Brigham KL, Rojas M, Bellamkonda RV, Johns MM, Laryngoscope 2010, 120, 988; [PubMed: 20422696] (b)Kamaly N, Yameen B, Wu J, Farokhzad OC, Chem. Rev 2016, 116, 2602. [PubMed: 26854975]
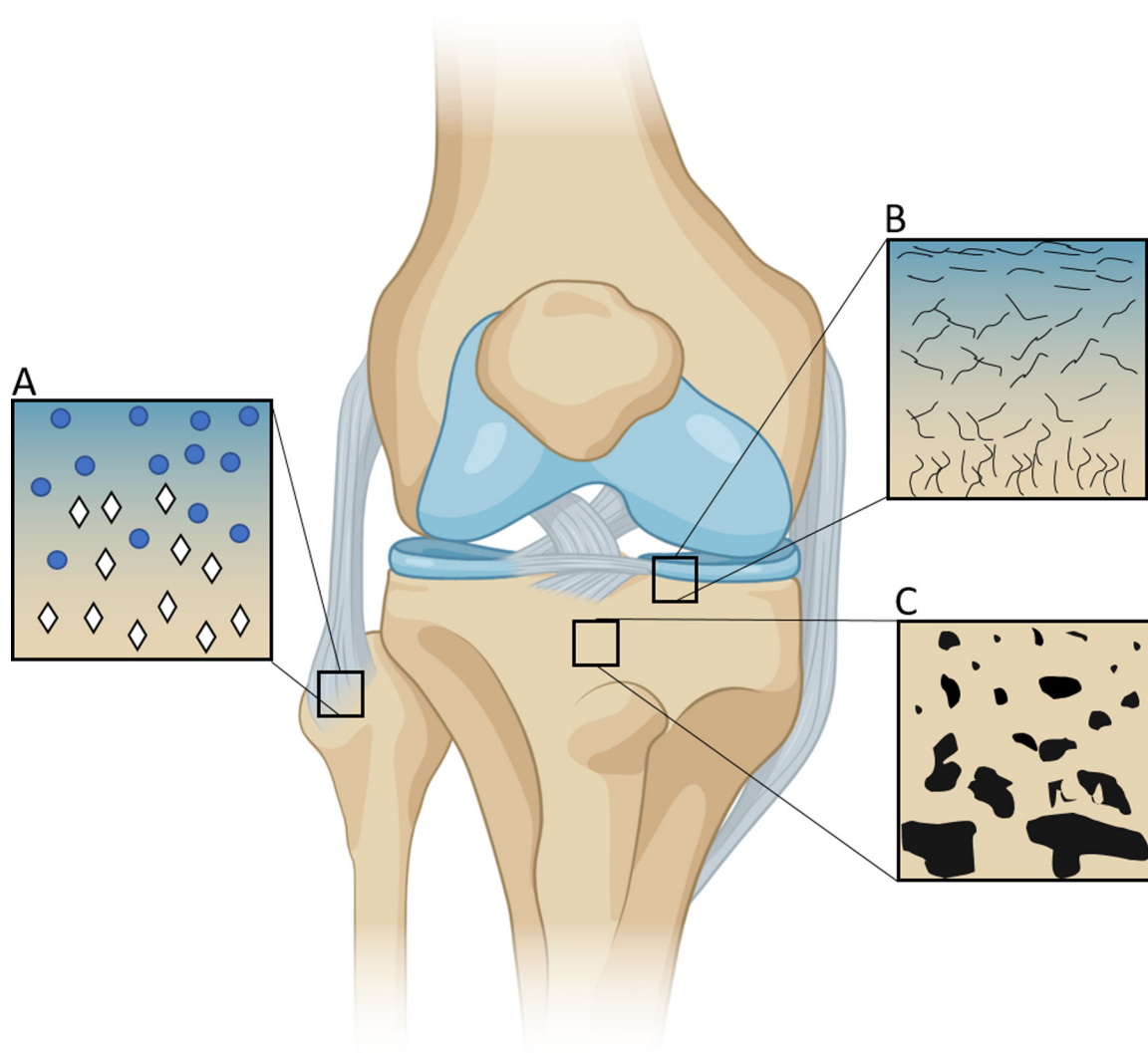
Figure 1. Native functional gradients enable tissues to withstand compressive and torsional forces and facilitate nutrient transport.
(A) Mineralization gradient as ligament inserts into bone at the enthesis. Blue circles depict fibroblasts while white rhombuses depict hydroxyapatite. **(B)** Gradient of collagen fiber alignment in articular cartilage illustrates parallel collagen fibers in the superficial zone that become perpendicularly aligned toward the subchondral bone. **(C)** Porosity gradient from cortical to trabecular bone facilitates a transition from high strength and toughness that provides protection from the external environment to a more porous network that is home to stem and progenitor cells and increased cell exchange and nutrient transport.
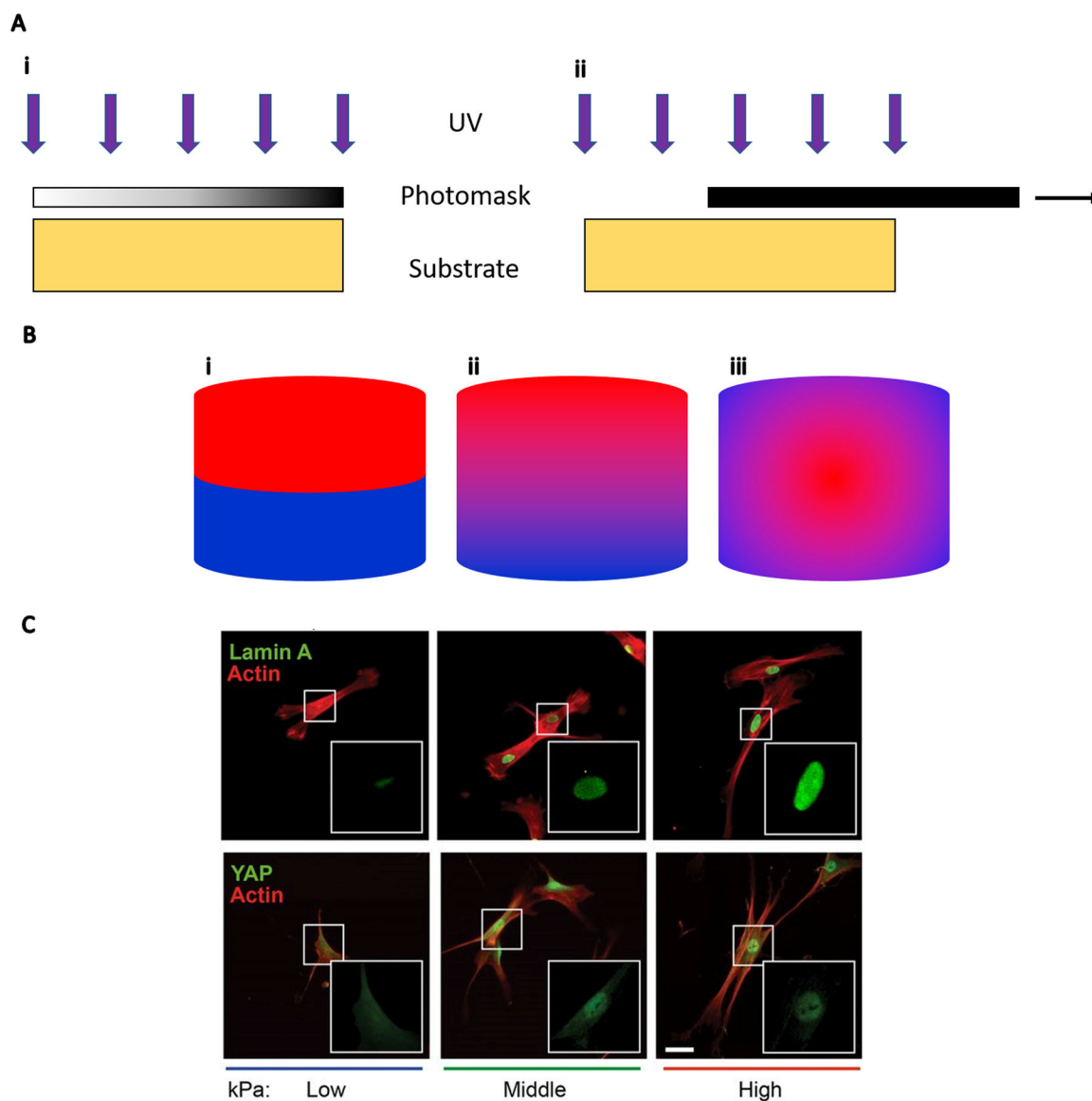
Figure 2.
(A) UV generation of continuous gradients with photomasks. (i) UV light penetrates a photomask with a gradient in translucency to create a linear gradient on the substrate below. **(ii)** A photomask is pulled across a substrate to create a spatiotemporal gradient of UV exposure time. **(B) Cross-sectional view of gradient patterns. (i)** Discrete linear gradient which is often a result of combining individually fabricated materials. **(ii)** Continuous linear gradient used to interrogate the relationship of continuous stiffness changes on cell adhesion or differentiation. **(iii)** Radial gradient. An example of a non-linear gradient such as oxygen tension within and surrounding a cell spheroid. **(C)** ASCs exhibit more spreading and nuclear localization of Lamin A and YAP as substrate stiffness increases from low (2 kPa) to high (40 kPa); scale bar = 50 μm. Panel C reprinted from Reference 13 with permission from the National Academy of Sciences.
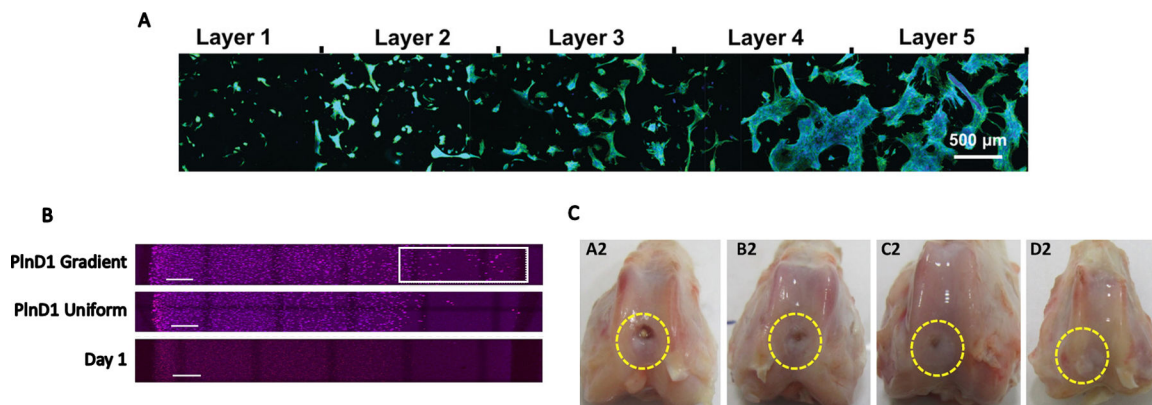
Figure 3. Cellular response to FGMs.
(A) ASCs exhibit increased spreading and proliferation as stiffness of annealed microgels increases from Layer 1 to Layer 5. Image reproduced from Reference 73 with permission from John Wiley and Sons. **(B)** MDA-MB-231 breast cancer cells exhibit increased migration by day 7 towards the region of interest (white box) on a perlecan domain I gradient compared to uniform perlecan distribution and a day 1 control, scale bar = 1mm. Reprinted from Reference 61 with permission from Elsevier. **(C)** Biphasic HAp and CS scaffolds (D2) outperformed monophasic CS (C2), HA (B2), and sham (A2) groups in a rabbit osteochondral defect model. Reprinted from Reference 133 with permission from Elsevier.
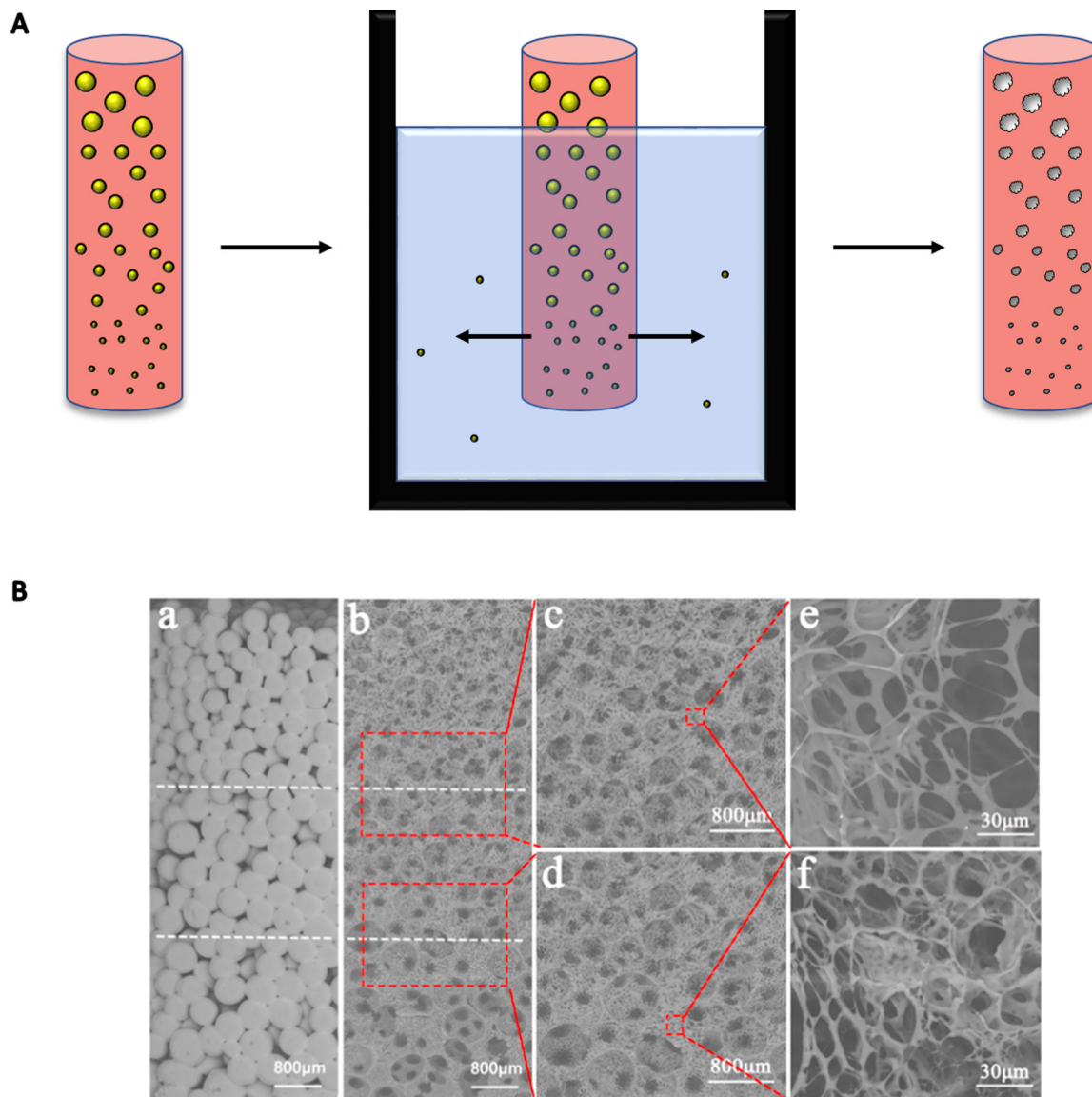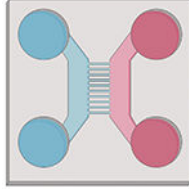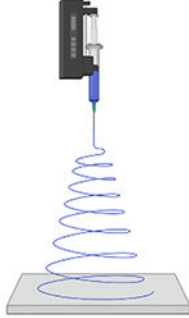
Figure 4.
(A) Porogens such as salt or sugar can be distributed in a scaffold by size and subsequently leached out to create a porosity gradient. This construct can model the porosity gradient in bone. Porogen is denoted as yellow spheres, while resulting pores are white with imperfect boundaries. **(B)** Sugar particles leached out of a PLLA scaffold created a gradient in pore size from 300 to 600 μm. Sugar particle gradient can be seen in part a, with the resultant porosity after leaching in part b. Parts c-f are higher magnification. Reprinted from Reference 114 with permission from Elsevier.

Table 1.

Methods for generating functional gradients in biomaterials.

Method		Advantages	Disadvantages
Light-based		• High resolution • Rapid manufacturing • Inexpensive	• Cytotoxicity • DNA damage
3D printing		• Rapid prototyping • Freedom of design	• Limited to "printable" material • Post-processing
Microfluidics		• Single cell handling • Reduced reagent consumption • Inexpensive	• Non-standard cell culture • Small volumes
Electrospinning		• Scalable • Inexpensive • Versatile	• Toxicity (solvents) • Extensive optimization required • Acellular

Table 2.

Applications of functionally graded materials.

Application	Composition		Gradient Type		Reference
Angiogenesis	•	6-bromo-7-hydroxy coumarin	•	Biochemical	[22]
	•	VEGF			
Cartilage	•	Poly(ε-caprolactone)	•	Mineralization	[41]
	•	Chondroitin sulfate	•	Adhesive	
	•	Bioactive glass			
Cartilage	•	Poly(ε-caprolactone)	•	Porosity	[42]
	•	Chitosan	•	Biochemical	
	•	Collagen			
Dural	•	Poly(ε-caprolactone)	•	Stiffness	[43]
	•	Collagen	•	Biochemical	
	•	Polylactic acid			
Neural growth	•	Poly(ε-caprolactone)	•	Biochemical	[37]
	•	IKVAV peptide			
Osteochondral	•	Hydroxyapatite	•	Mineralization	[44]
	•	Poly(ε-caprolactone)	•	Porosity	
Osteochondral	•	Alginate	•	Porosity	[45]
	•	Methylcellulose			
Osteochondral	•	β-tricalcium phosphate	•	Stiffness	[46]
	•	TGF-β1	•	Biochemical	
	•	Poly(N-acryloyl glycinamide)			
Osteochondral	•	Silk fibroin	•	Mineralization	[47]
	•	Silk-CaP			
Tendon-to-bone	•	Poly(lactic co-glycolic acid)	•	Stiffness	[48]
	•	Simulated body fluid	•	Mineralization	
Tendon-to-bone	•	Collagen	•	Alignment	[49]
	•	Glycosaminoglycans	•	Biochemical	